

Are magnetite (Fe_3O_4) films on MgAl_2O_4 auxetic?

M. Ziese*

Abteilung Supraleitung und Magnetismus, Universität Leipzig, D-04103 Leipzig, Germany

(Dated: June 20, 2018)

Magnetite (Fe_3O_4) films were fabricated on MgAl_2O_4 (001) single crystal substrates by pulsed laser deposition. In-plane and out-of-plane lattice constants were determined by X-ray diffraction. The apparent Poisson's ratio was determined as the negative ratio of the out-of-plane to in-plane strains. The results show that (i) the determination of Poisson's ratio by this method is only reliable for fully strained films and (ii) Poisson's ratio $\nu_{100} \simeq 0.3$ along the $\langle 100 \rangle$ direction is positive for this archetypal ferrite. Fe_3O_4 films grown on MgAl_2O_4 (001) are not auxetic.

PACS numbers: 62.20.dj, 75.47.Lx, 75.70.Ak, 81.40.Jj

Auxetic materials are substances with a negative Poisson ratio, i.e. these expand in the transverse direction when stretched and contract when compressed [1]. This behavior is often found in foams and organic material such as cartilage, where it is related to the microstructure and the appearance of so-called re-entrant cells [2]. Although counterintuitive, auxetic behavior does not violate thermodynamic principles, since the non-negativity of the elastic constants restricts the possible values for Poisson's ratio ν in isotropic materials to the range of values $-1 < \nu < 0.5$. In anisotropic media the situation is more complicated, since Poisson's ratio depends in an intricate way on the values of the elastic moduli C_{ij} as well as on the directions of the longitudinal stress and transverse strain. For cubic materials this has been studied in detail [3–9]. In case of Poisson's ratio in the $\langle 100 \rangle$ direction, which is of interest here, one obtains

$$\nu_{100} = \frac{C_{12}}{C_{11} + C_{12}}. \quad (1)$$

With the stability criteria, see e.g. [9, 10], $C_{11} > 0$, $-C_{11}/2 < C_{12} < C_{11}$ and $C_{44} > 0$, one again obtains $-1 < \nu_{100} < 0.5$ as for isotropic materials. In general, however, Poisson's ratio can have smaller or larger values than these for general directions in the crystal [5–9], especially for directions close to the $\langle 111 \rangle$ direction [8].

Recently molecular auxetic behavior in epitaxial cobalt ferrite films grown on SrTiO_3 (001) substrates as determined by X-ray diffraction measurements of the in-plane and out-of-plane strains was reported [11]. This observation was interpreted in terms of the atomic spinel structure, but not related to the specific microstructure of the films. Since various ferrites crystallize in the spinel structure, especially the parent compound magnetite (Fe_3O_4), it is tempting to search for auxetic behavior in magnetite films.

Magnetite films were grown by pulsed laser deposition from stoichiometric polycrystalline targets onto MgAl_2O_4 (001) substrates. Deposition conditions were a substrate temperature T_{sub} between 370 and 530°C and an oxygen partial pressure between 7×10^{-7} mbar and 1.5×10^{-5} mbar. An excimer laser (Lambda Physik) op-

erating at a wavelength of 248 nm (KrF), a repetition rate of 10 Hz and a fluence of about 1.5 J/cm^2 was used for the ablation. The thickness of the films was measured with a Dektak surface profile measuring system. Structural characterization of the films was made by X-ray diffraction (XRD) with a Philips X'pert system using Cu K_α radiation. Both $\theta - 2\theta$ scans as well as reciprocal space maps of the (226) reflections were recorded. Magnetic characterization of the films was made by SQUID magnetometry (Quantum Design model MPMS-7). For further details on film growth and characterization see [12].

Two series of films with thicknesses between 25 nm and 240 nm (series I) as well as between 10 nm and 160 nm (series II) were studied. The bulk lattice constant of the cubic phase of magnetite at room temperature is $a_b = 0.8398$ nm, the lattice constant of MgAl_2O_4 is $a_s = 0.8084$ nm, respectively. The lattice mismatch is -3.7% and, accordingly, the films are expected to be under compressive in-plane strain. Out-of-plane lattice constants a_\perp were determined from $\theta - 2\theta$ scans, in-plane lattice constants a_\parallel from reciprocal space maps of the (226) reflection. Out-of-plane and in-plane strains were calculated from

$$\epsilon_\perp = \frac{a_\perp - a_b}{a_b} \quad (2)$$

$$\epsilon_\parallel = \frac{a_\parallel - a_b}{a_b}, \quad (3)$$

and the degree of relaxation was defined as

$$R = \frac{a_\parallel - a_s}{a_b - a_s}. \quad (4)$$

The results of the X-ray analysis are presented in table I and are illustrated in Fig. 1. Although for all films the volume is smaller than the bulk volume, the in-plane strain is negative and compressive, whereas the out-of-plane strain is positive and tensile. The thinnest films of each series are fully strained, but thicker films show considerable strain relaxation approaching almost 100%, see Fig. 1(b) (left scale). The films of series II were grown under identical conditions for substrate temperature and

TABLE I. Results of the X-ray analysis. Parallel a_{\parallel} and perpendicular a_{\perp} lattice constants were determined from reciprocal space maps and $\theta - 2\theta$ scans, respectively. In-plane strain ϵ_{\parallel} , out-of-plane strain ϵ_{\perp} , degree of relaxation R , volume change $\Delta V/V = (a_{\parallel}^2 a_{\perp} - a_b^3)/a_b^3$ and apparent Poisson ratio $\nu^* = -\epsilon_{\perp}/\epsilon_{\parallel}$ were calculated from the lattice constants. Film thickness t and oxygen pressure p_{O_2} during deposition are also shown.

t (nm)	T_s ($^{\circ}\text{C}$)	p_{O_2} (mbar)	a_{\parallel} (nm)	a_{\perp} (nm)	R (%)	ϵ_{\parallel} (%)	ϵ_{\perp} (%)	$\frac{\Delta V}{V}$ (%)	ν^*
Series I									
25	530	3×10^{-6}	-	-	-	-	-	-	-
35	500	3×10^{-6}	0.8084	0.8494	0	-3.74	1.14	-6.29	0.31
80	450	1.5×10^{-5}	0.8272	0.8431	0.60	-1.50	0.39	-2.60	0.26
90	450	7×10^{-7}	0.8231	0.8503	0.47	-1.99	1.25	-2.74	0.63
155	450	3×10^{-6}	0.8369	0.8452	0.91	-0.35	0.64	-0.05	1.86
165	370	1.5×10^{-5}	0.8354	0.8444	0.86	-0.52	0.55	-0.50	1.05
240	370	3×10^{-5}	-	-	-	-	-	-	-
Series II									
10	450	3×10^{-6}	0.8084	0.8498	0	-3.74	1.19	-6.25	0.32
20	450	3×10^{-6}	0.8136	0.8475	0.17	-3.12	0.92	-5.28	0.29
30	450	3×10^{-6}	0.8310	0.8480	0.72	-1.05	0.98	-1.13	0.93
80	450	3×10^{-6}	0.8341	0.8462	0.82	-0.68	0.76	-0.60	1.12
160	450	3×10^{-6}	0.8316	0.8428	0.74	-0.98	0.36	-1.59	0.37

oxygen partial pressure, whereas both parameters were varied for the films of series I. This might explain that the thickness at which strain relaxation sets in, is significantly different. However, the strain state is controlled by many factors such as fluence, growth rate and substrate quality that are not at all times exactly reproduced.

The apparent Poisson ratio was defined as [11]

$$\nu^* = -\frac{\epsilon_{\perp}}{\epsilon_{\parallel}}. \quad (5)$$

This is presented in table I and shown in Fig. 1(b) (right scale). The apparent Poisson ratio is positive for all film thicknesses studied here. For the fully strained films a conventional value around 0.3 is obtained, whereas in relaxed films unphysically large values were found. This is reasonable, since the strain state in a relaxed film is certainly inhomogeneous such that the definition of the Poisson ratio via averaged strain values is not valid. Literature values for the elastic moduli with C_{11} , $C_{12} = 270$, 108 GPa [13], 268, 106 GPa [14], 260, 148 GPa [15], and 312, 184 GPa [16] yield Poisson ratios $\nu_{100} = 0.29$, 0.28, 0.36, and 0.37. These values are in good agreement with the value obtained here for the fully strained films.

One problem in the growth of oxide films lies in the stabilization of the correct oxygen stoichiometry. Oxygen stoichiometry was indirectly assessed in the films by the measurement of the Verwey temperature, i.e. the transition temperature of the transformation from the high temperature cubic into the low temperature monoclinic phase. The Verwey temperature sensitively depends on the oxygen stoichiometry [17]. Fig. 2 shows (a) the normalized magnetic moment m and (b) its derivative dm/dT of the fully strained and strain relaxed films from series II with thicknesses of 20 nm and 160 nm, respectively. The thick film showed a single transition at the Verwey temperature of 114 K, whereas the thin film

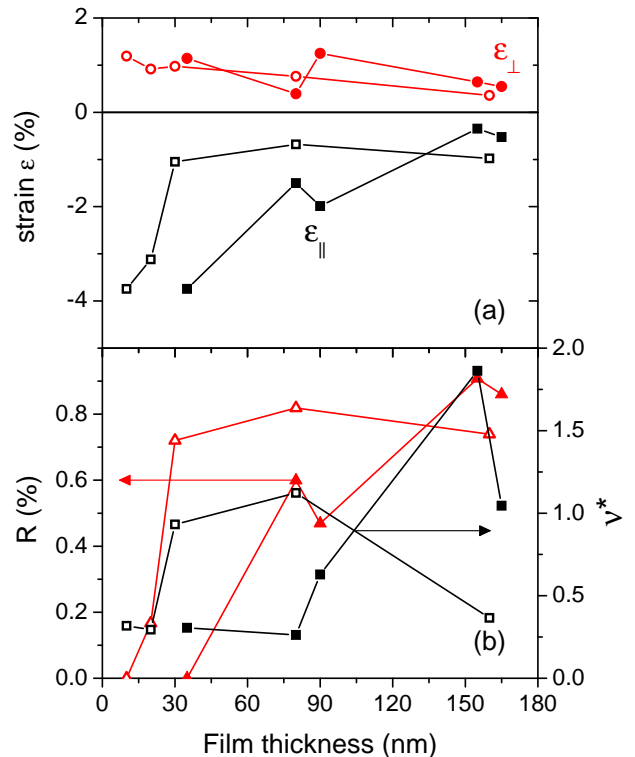


FIG. 1. (Color online) (a) In-plane ϵ_{\parallel} and out-of-plane ϵ_{\perp} strain as a function of film thickness. (b) Degree of relaxation R (red triangles, left axis) and apparent Poisson's ratio ν^* (black squares, right axis) as a function of film thickness. Solid symbols: series I, open symbols: series II.

showed a double transition (most clearly seen by the two peaks in the derivative dm/dT) with Verwey temperatures of 122.8 and 105.4 K. Except for the thickest film all films of series II showed a double transition, whereas all films from series I showed a single transition. The cor-

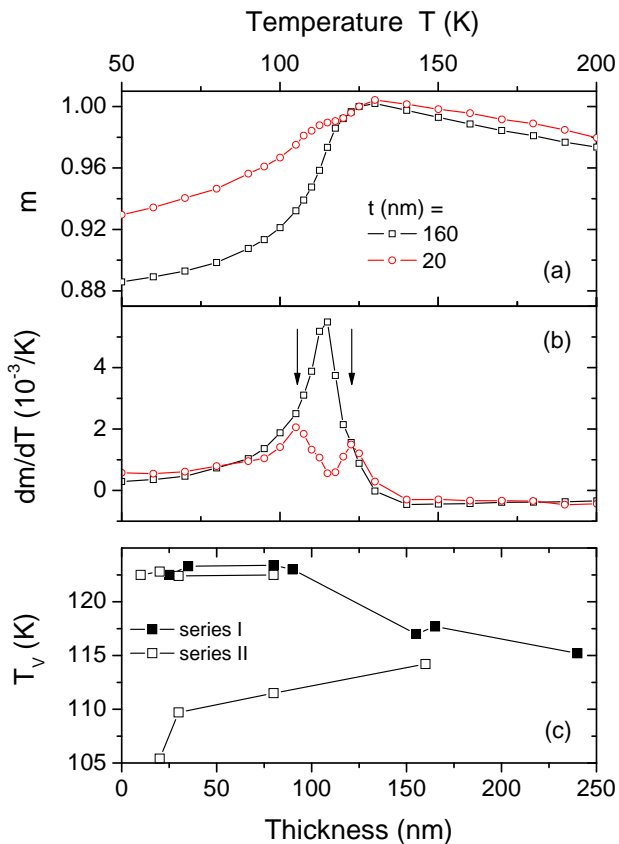


FIG. 2. (Color online) (a) Magnetic moment of the 20 nm and 160 nm magnetite films of series II normalized to the value at 130 K. (b) Temperature derivative of the normalized magnetic moment. The maxima indicate the Verwey temperature T_V . (c) Verwey temperature T_V vs. film thickness.

responding Verwey temperatures are shown in Fig. 2(c) as a function of thickness. There are two trends: with decreasing thickness the Verwey transition temperature of most of the films increases to a value near 123 K which is close to the bulk value of 125 K; if a double transition is present, the lower transition temperature decreases with decreasing film thickness. The latter behavior was reported before and was related to strain effects [18–21]. The present data indicate that – even if the films appear fully strained in X-ray diffractometry measurements – some films might be in an inhomogeneous strain state with a magnetite layer with high Verwey temperature adjacent to the substrate and another layer with lower Verwey temperature and probably different microstructure on top of the first layer. Without further structural investigations it is impossible to determine whether strain, microstructural effects or deoxygenation is the main factor determining the value of the Verwey temperature and its dependence on the film thickness. Overall, however, the Verwey temperature of the thin films is close to the bulk value indicating a nearly ideal oxygen stoichiometry.

The results presented here show that magnetite films

grown on $MgAl_2O_4$ are not auxetic, at least not along the $\langle 100 \rangle$ direction. Poisson’s ratio $\nu^* = 0.3$ determined from the in-plane and out-of-plane strain ratio of a fully strained film is in good agreement with the value derived from measurements of the elastic moduli. Since both magnetite and cobalt ferrite crystallize in the inverse spinel structure, these data cast doubt on the claim of molecular auxetic behavior in cobalt ferrite films grown on $SrTiO_3$ (001) [11]. Indeed, using the experimentally measured elastic moduli of cobalt ferrite, $C_{11} = 257$ GPa, $C_{12} = 150$ GPa [14], or the calculated values $C_{11} = 240 - 282$ GPa, $C_{12} = 137 - 168$ GPa [22], a positive Poisson’s ratio $\nu_{100} = 0.37$ is obtained that is incompatible with auxetic behavior. A similar conclusion against auxetic behaviour was reached in [23] for $NiFe_2O_4$ films on $MgAl_2O_4$. The data presented here clearly show that Poisson’s ratio can be reliably determined from X-ray measurements on fully strained films.

This work was supported by the DFG within SFB 762 “Functionality of Oxide Interfaces”. I thank H. C. Semmelhack for the X-ray diffractometry and R. Höhne for the magnetization measurements.

* ziese@physik.uni-leipzig.de

- [1] R. S. Lakes, *Science* **235**, 1038 (1987).
- [2] R. Lakes, *J. Materials Science* **26**, 2287 (1991).
- [3] J. Turley and G. Sines, *J. Phys. D: Appl. Phys.* **4**, 264 (1971).
- [4] D. J. Gunton and G. A. Saunders, *Proc. R. Soc.* **343**, 68 (1975).
- [5] S. P. Tokmakova, *phys. stat. sol. (b)* **242**, 721 (2005).
- [6] T. C. T. Ting and D. M. Barnett, *J. Appl. Mech. ASME* **72**, 929 (2005).
- [7] K. W. Wojciechowski, *Comp. Methods Sci. Technol.* **11**, 73 (2005).
- [8] A. N. Norris, *Proc. R. Soc. A* **462**, 3385 (2006).
- [9] T. Paszkiewicz and S. Wolski, *phys. stat. sol. (b)* **244**, 966 (2007).
- [10] L. D. Landau and E. M. Lifshitz, *Elastizitätstheorie* (Verlag Harri Deutsch, 1991).
- [11] M. Valant, A.-K. Axelsson, F. Aguesse, and N. M. Alford, *Adv. Func. Mater.* **20**, 644 (2010).
- [12] A. Bollero, M. Ziese, R. Höhne, H. C. Semmelhack, U. Köhler, A. Setzer, and P. Esquinazi, *J. Magn. Magn. Mater.* **285**, 279 (2005).
- [13] P. K. Baltzer, *Phys. Rev.* **108**, 580 (1957).
- [14] Z. Li, E. S. Fisher, J. Z. Liu, and M. V. Nevitt, *J. Mater Science* **26**, 2621 (1991).
- [15] H. J. Reichmann and S. D. Jacobsen, *Am. Mineralogist* **89**, 1061 (2004).
- [16] D. Chicot, F. Roudet, A. Zaoui, G. Louis, and V. Lepage, *Mater. Chem. Phys.* **119**, 75 (2010).
- [17] Z. Kakol and J. M. Honig, *Phys. Rev. B* **40**, 9090 (1989).
- [18] R. A. Lindley, S. P. Sena, H. J. Blythe, and G. Gehring, *J. Phys. IV France* **7**, C1 (1997).
- [19] S. P. Sena, R. A. Lindley, H. J. Blythe, C. Sauer, M. Al-Kafarji, and G. A. Gehring, *J. Magn. Magn. Mater.* **176**,

- 111 (1997).
- [20] S. K. Arora, R. G. S. Sofin, I. V. Shvets, and M. Luysberg, *J. Appl. Phys.* **100**, 073908 (2006).
- [21] J. Orna, P. A. Algarabel, L. Morellón, J. A. Pardo, J. M. de Teresa, R. L. Antón, F. Bartolomé, L. M. García, J. Bartolomé, J. C. Cezar, and A. Wildes, *Phys. Rev. B* **81**, 144420 (2010).
- [22] D. Fritsch and C. Ederer, *Phys. Rev. B* **82**, 104117 (2010).
- [23] M. N. Iliev, D. Mazumdar, J. X. Ma, A. Gupta, F. Rigato, and J. Fontcuberta, *Phys. Rev. B* **83**, 014108 (2011).